ELSEVIER

Available online at www.sciencedirect.com

SCIENCE DIRECT®

Theoretical Computer Science 319 (2004) 71–81

Theoretical Computer Science

www.elsevier.com/locate/tcs

A formula for the number of tilings of an octagon by rhombi

N. Destainville[a,*], R. Mosseri[b], F. Bailly[c]

[a] *Laboratoire de Physique Théorique-IRSAMC, UMR CNRS/UPS 5152, Université Paul Sabatier, 118, route de Narbonne, Toulouse 31062 Cedex 04, France*

[b] *Groupe de Physique des Solides, CNRS et Université Paris 6, Campus Boucicaut, 140 Rue de Lourmel, Paris 75015, France*

[c] *Laboratoire de Physique du Solide-CNRS, 1, place Aristide Briand, Meudon 92195 Cedex, France*

Abstract

We propose the first algebraic determinantal formula to enumerate tilings of a centro-symmetric octagon of any size by rhombi. This result uses the Gessel–Viennot technique and generalizes to any octagon a formula given by Elnitsky in a special case.

Keywords: Exact enumeration; Rhombus tilings; Random tilings; Centro-symmetric octagon; Gessel–Viennot method

0. Introduction

The enumeration of tilings of a centro-symmetric polygon by rhombi is a notoriously difficult problem that concerns discrete mathematics and theoretical computer science, as well as theoretical physics, in relation with quasicrystallography. In the latter community, these tilings are usually called "random tilings with octagonal symmetry". We address the following issue: given a centro-symmetric octagon $O_{a,b,c,d}$, of integral sides lengths a, b, c and d (read clockwise; see Fig. 2, left), in how many ways is it possible to fill it entirely, without any gap or overlap, with the following six species of tiles: two differently oriented squares, and four differently oriented 45° rhombi, the six of them with unitary side lengths? So far, this question has been solved in very particular instances only. We denote by $\mathcal{T}_{a,b,c,d}$ the set of all the tilings of $O_{a,b,c,d}$, and by

* Corresponding author.
E-mail address: destain@irsamc.ups-tlse.fr (N. Destainville).

0304-3975/$ - see front matter
doi:10.1016/j.tcs.2004.02.025

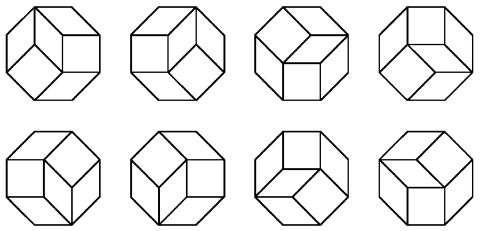

Fig. 1. The eight tilings of the set $\mathscr{T}_{1,1,1,1}$.

Table 1
Some tiling enumerations computed in Ref. [4]. The number of rhombi is given in column 3

a,b,c,d	$T_{a,b,c,d}$	No. of tiles
1, 1, 1, 1	8 (see Fig. 1)	6
2, 2, 2, 2	5383	24
3, 3, 3, 3	273976272	54
4, 4, 4, 4	1043065776718923	96
5, 5, 5, 5	296755610108278480324496	150

$T_{a,b,c,d} = |\mathscr{T}_{a,b,c,d}|$ the cardinality of $\mathscr{T}_{a,b,c,d}$. For example, Fig. 1 displays the eight tilings of the set $\mathscr{T}_{1,1,1,1}$.

Small systems have been studied in Refs. [4,11] up to sizes of some hundred tiles (see Table 1). However, the technique employed cannot reasonably provide tiling enumerations for bigger octagons. On the other hand, Elnitsky gave in Ref. [6] two formulas when two sides of the octagon are set to 1:

$$T_{a,1,c,1} = \sum_{r+s=a} \sum_{t+u=c} \binom{r+t}{r} \binom{s+t}{s} \binom{r+u}{r} \binom{s+u}{s} \tag{1}$$

and

$$T_{a,b,1,1} = \frac{2(a+b+1)!\,(a+b+2)!}{a!\,b!\,(a+2)!\,(b+2)!}. \tag{2}$$

The first formula has been later partially simplified [4]:

$$T_{a,1,c,1} = \frac{(a+c+1)!}{a!\,c!\,(2a+1)(2c+1)} \left[\frac{2(a+c+1)!}{a!\,c!} + \sum_{k=0}^{a} \frac{1}{2k-1} \binom{a}{k} \binom{c}{k} \right], \tag{3}$$

where the last sum can be written in terms of a hypergeometric function

$$\sum_{k=0}^{a} \frac{1}{2k-1} \binom{a}{k} \binom{c}{k} = {}_3F_2[-1/2, -a, -c; 1/2, 1; 1]. \tag{4}$$

We propose a generalization of the first formula (1) to any side lengths, where $T_{a,b,c,d}$ is written as a sum of products of determinants. Even if the complexity of our formula

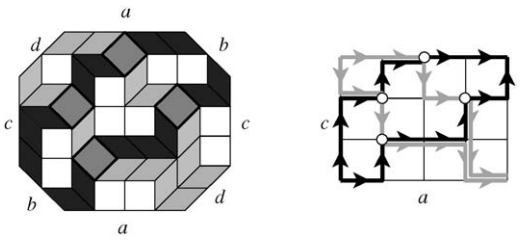

Fig. 2. Left: example of octagonal tiling of a centro-symmetric octagon of sides a, b, c, d. There are 6 species of tiles with unitary side length: two squares and four 45° rhombi. One species of squares, the "tilted" squares, is emphasized in medium gray. They lie at the intersections of the light gray and dark gray de Bruijn lines. De Bruijn lines are defined in Section 1 and are made up of adjacent rhombi sharing an edge with a given orientation. Right: square grid representation of the same tiling, obtained by shrinking all colored tiles; see Section 1. The white disks on the grid keep track of the position of the tilted squares of the original tiling. The orientation of edges (arrows) will be discussed later.

increases with the system size, it is the first explicit algebraic expression to count tilings of an octagon (see Eq. (12)), which can be in principle calculated for any system size.

As it is discussed below into detail, Elnitsky's proof uses a "square grid representation" of tilings (see Fig. 2), which is closely related to the "de Bruijn dualization", a wide-spread technique in quasicrystal science. This dualization has proved powerful to handle rhombus tilings in several circumstances. The present paper also uses this technique, thus generalizing Elnitsky's proof.

We now state our main result. Given the side lengths a, b, c and d, we denote by X (resp. Y) the set of families of integers $(x_{k,l})$ (resp. $(y_{k,l})$), $k = 1,\ldots,b$, $l = 1,\ldots,d$, satisfying the relations:

$$0 \leqslant x_{k,l} \leqslant a, \tag{5}$$

$$x_{k,l} \leqslant x_{k',l'} \quad \text{if } k \leqslant k' \text{ and } l \leqslant l', \tag{6}$$

$$0 \leqslant y_{k,l} \leqslant c, \tag{7}$$

$$y_{k,l} \leqslant y_{k',l'} \quad \text{if } k \geqslant k' \text{ and } l \leqslant l'. \tag{8}$$

Note that conditions (6) and (8) are not exactly similar. In the following, these integers will be the coordinates of the white disks in the grid representation (see Fig. 2, right, and Section 1). In addition, we set by convention for $k = 1,\ldots,b$ and $l = 1,\ldots,d$

$$\begin{aligned} &x_{k,0} = 0, \quad y_{k,0} = 0,\\ &x_{0,l} = 0, \quad y_{0,l} = c,\\ &x_{b+1,l} = a, \quad y_{b+1,l} = 0,\\ &x_{k,d+1} = a, \quad y_{k,d+1} = c. \end{aligned} \tag{9}$$

The reasons for this convention will be explicited below. For any two such sequences $x=(x_{k,l})$ and $y=(y_{k,l})$, we define the matrices $M^{(u)}(x,y)$ and $P^{(v)}(x,y)$ as follows: $M^{(u)}(x,y)$ is a $b\times b$ matrix of coefficients

$$m_{ij}=\begin{pmatrix} x_{j,u}-x_{i,u-1}+y_{j,u}-y_{i,u-1} \\ x_{j,u}-x_{i,u-1}+j-i \end{pmatrix} \tag{10}$$

for $1\leqslant i,j\leqslant b$ and $P^{(v)}(x,y)$ is a $d\times d$ matrix of coefficients

$$p_{ij}=\begin{pmatrix} x_{v,j}-x_{v-1,i}+y_{v-1,i}-y_{v,j} \\ x_{v,j}-x_{v-1,i}+j-i \end{pmatrix} \tag{11}$$

for $1\leqslant i,j\leqslant d$. Note that, by convention, we set $\binom{A}{B}=0$ whenever $A<0$ or $B<0$ or $B>A$.

Theorem 1. *With the previous notations, the number of rhombus tilings of a centrosymmetric octagon of sides a,b,c,d reads*:

$$T_{a,b,c,d}=\sum_{(x,y)\in X\times Y}\prod_{u=1}^{d+1}\det M^{(u)}(x,y)\prod_{v=1}^{b+1}\det P^{(v)}(x,y). \tag{12}$$

It is demonstrated below that the determinants come from the enumeration, by the Gessel–Viennot method (presented below), of tilings of independent sub-domains of the octagon delimited by some points of coordinates $(x_{k,l},y_{k,l})$ in the square grid representation.

When $b=d=1$, the previous expression is reduced to Elsnitsky's relation (1). Note that by contrast, relation (2) is *not* a spacial case of this formula. Beyond this simple case, the number of terms in the formula grows with the octagon size. For example, for $(a,b,c,d)=(2,2,2,1)$, the formula contains $6\times 6=36$ terms to count the 480 tilings. For $(a,b,c,d)=(2,2,2,2)$, there are $20\times 20=400$ terms and 5383 tilings. More generally, the number of terms grows exponentially with the number of tiles, but it nevertheless grows exponentially more slowly than the number of tilings. As a consequence, this formula is exponentially more compact than the crude enumeration of tilings. This point is discussed in the conclusion.

1. Octagonal tilings and the square grid representation

In this section, we show that octagonal tilings are conveniently represented by families of directed paths running on a rectangular patch of square grid. This representation was used by Elnitsky [6] and it is reminiscent of the prior "de Bruijn dualization" [1,2,8,12] and derived representations [4,11]. We first expose briefly the de Bruijn dualization process. Figs. 2 and 3 will help the reader. To begin with, we notice that tile edges can have four possible orientations. We define a *family of de Bruijn lines* for each orientation: de Bruijn lines are made up of adjacent rhombi sharing an edge with

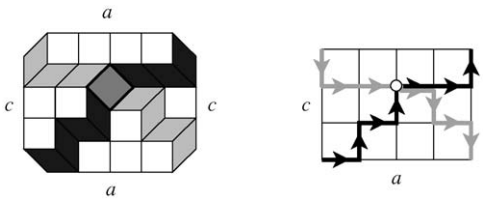

Fig. 3. Example of tiling in the case $b=d=1$ (left) together with its square grid representation (right). We have emphasized two de Bruijn lines of the tiling, belonging to two different families. Their intersection coincides with the gray tilted square. They are represented by two directed paths joining two opposite corners of the grid. These paths can have multiple intersections. To avoid ambiguity on the position of the gray tilted square on the original tiling, a white circle marks a *distinguished* vertex to keep track of its position on the grid. Note that when two paths are tangent, we have slightly shifted one of them for the sake of readability. However, these paths are in fact superimposed and lie on the same grid edge.

this orientation. It is always possible to extend these lines through the whole tiling up to a boundary tile. Two examples of lines are presented in both Figs. 2 and 3, belonging to two different families. A rhombic tile is situated at the intersection of two lines of different families (see the figures). By construction, lines of a same family never intersect; there are respectively a, b, c and d lines in each family.

Now we show how to translate the de Bruijn's representation of a tiling into its square grid representation. In Fig. 3, we show this correspondence in the simplest case $b=d=1$ [6]. The idea is to shrink the de Bruijn lines of two families among four, so that they become paths on a square grid, as displayed in Figs. 2 or 3. Because all tiles of a de Bruijn line have an edge of a given orientation, these paths are directed. The b paths of the first family (denoted by SW) go from the south-west corner to the north-east one (dark gray); they can follow eastward and northward edges only; the d paths of the second family (denoted by NW) go from the north-west corner to the south-east one (light gray); they can follow eastward and southward edges only.

In the simplest case $b=d=1$, to avoid ambiguity due to path tangency and to make this correspondence bijective [6], we keep track of the intersection of the de Bruijn lines thanks to a *distinguished vertex*, represented by a white disk in the right figure. It marks the position of the unique tilted square (medium gray). When $b>1$ or $d>1$ as in Fig. 2, there are bd intersections and therefore bd tilted squares. Each of them must be located by a distinguished vertex on the square grid. Paths do not cross in a same family even though *they can be locally adjacent* (see Fig. 2). We denote the paths of SW (resp. NW) by $SW_1,\ldots,SW_b$ (resp. $NW_1,\ldots,NW_d$) from left to right. As a consequence, distinguished vertices are indexed by two integers k and l, and are denoted by $DV_{k,l}$ (see Fig. 4).

2. The Gessel–Viennot method

The Gessel–Viennot method [9,13] is a combinatorial technique for the counting of configurations of directed non-intersecting paths on oriented graphs. This technique

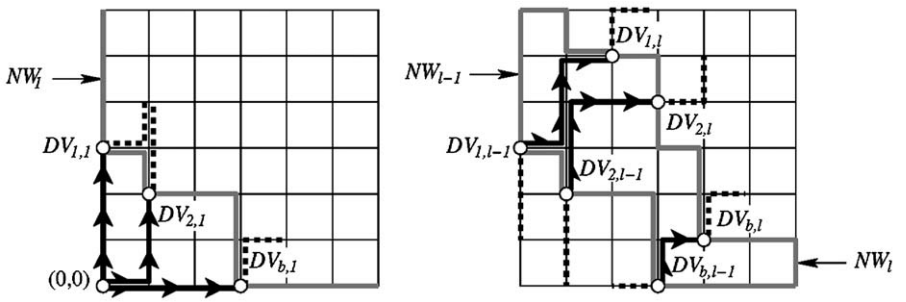

Fig. 4. Examples of configurations of non-crossing directed paths, belonging to the sets $sw(1)$ (left) and $sw(l)$ (right). Each path (solid black lines) is a section of a path SW_k and goes from $DV_{k,l-1}$ to $DV_{k,l}$ (white circles). By convention, $DV_{k,0}=(0,0)$. The gray paths NW_1, NW_{l-1} and NW_l do not belong to the path configurations and are drawn for information only. The dashed black lines represent the possible continuations of the original paths SW_k. In this figure also, we have slightly shifted tangent paths for the sake of readability, whereas in reality they run on the same grid edge.

has already proved very useful for the enumeration of rhombus tilings (see [3,6] for examples, as well as Section 3 of the present paper). It has been extensively described in the literature [9,13] and we shall only briefly explain it in the present paper, focusing on the underlying ideas and not on technical details. The method is rather general and can be applied to any acyclic oriented graph $\mathscr{G}$, in which are selected two families of vertices, d_i ("departure" vertices) and a_j ("arrival" vertices), $i,j=1,\ldots,n$. We consider directed paths, running on $\mathscr{G}$, starting from one vertex d_i and arriving at one vertex a_j. By "directed", we naturally mean that the paths must follow the edge orientations. In addition, this graph is supposed to satisfy the property of *compatibility*: if two directed paths on $\mathscr{G}$ are going respectively from d_{i_1} to a_{j_1} and from d_{i_2} to a_{j_2}, if these paths do not cross, and if $i_1<i_2$ then $j_1<j_2$. This property is very specific to two-dimensional graphs.

We are interested in the number D_n of configurations of n non-intersecting directed paths on $\mathscr{G}$, where the ith path goes from d_i to a_i: two paths are said to be non-intersecting if they share no vertex; n paths are said to be non-intersecting if any two paths are non-intersecting. If we denote by λ_{ij} the number of paths going from d_i to a_j, then the Gessel–Viennot theorem states that

$$D_n=\det(\lambda_{ij})_{1\leqslant i,j\leqslant n}. \tag{13}$$

The idea of the proof is that in this determinant, all configurations of n paths, whether intersecting or not, the ith path going from d_i to $a_{\sigma(i)}$, for any permutation σ, are counted, with a $+$ or $-$ sign. Because of these signs, all configurations with one or more intersections cancel two by two. Only the non-intersecting configurations remain. They are exactly the configurations under interest thanks to the property of compatibility. The interested reader is referred to Stembridge [13] for more detailed explanations.

3. Proof of Theorem 1

We are now ready to prove Theorem 1. First of all, we need to endow the square grid with integer coordinates in order to locate the positions of distinguished vertices. They are defined according to the usual conventions, so that the south-west and north-east corners have respective coordinates $(0,0)$ and (a,c). The coordinates of $DV_{k,l}$ are denoted by $(x_{k,l}, y_{k,l})$. By extension, we also define the vertices $DV_{k,0}=(0,0)$, $DV_{k,d+1}=(a,c)$, $DV_{0,l}=(0,c)$ and $DV_{b+1,l}=(a,0)$. They are the ends of paths of families SW and NW. If their coordinates are also denoted by $(x_{k,l}, y_{k,l})$, these last definitions are compatible with conventions (9) given in introduction. All these coordinates naturally obey relations (5) and (7).

Furthermore, because of the directed character of de Bruijn lines, distinguished vertices $DV_{k,l}$ are constrained by some conditions when they belong to the same paths, and they must obey relations (6) and (8) as well. These four conditions define the sets X and Y, as it was stated in the introductory part.

Let $x=(x_{k,l})\in X$ and $y=(y_{k,l})\in Y$ be an admissible set of coordinates of the distinguished vertices. We denote by $\mathscr{T}_{x,y}$ the subset of tilings of $\mathscr{T}_{a,b,c,d}$ in the square grid representations of which the distinguished vertices have these coordinates. The subsets $\mathscr{T}_{x,y}$ are two-by-two disjoint so that $T_{a,b,c,d}=\sum_{(x,y)\in X\times Y}|\mathscr{T}_{x,y}|$. Our purpose is now to calculate each $|\mathscr{T}_{x,y}|$. This calculation is feasible because for a given (x,y), the subset $\mathscr{T}_{x,y}$ can be factorized into simple sets (see Eq. (15)). Each of them can in turn be counted by the Gessel–Viennot method, which leads to relation (12).

First we need to introduce two definitions. Given a configuration of vertices $DV_{k,l}=(x_{k,l}, y_{k,l})$, we fix l and we consider in isolation the vertices $DV_{k,l-1}$ as well as $DV_{k,l}$, $k=1,\ldots,b$ (see Figs. 4 and 5). Then we define the set $sw(l)$ of *all* the configurations of b directed non-crossing paths, the kth path going from $DV_{k,l-1}$ to $DV_{k,l}$, with $k=1,\ldots,b$. These paths are directed from south-west to north-east. They have no constraint except that they are directed and non-crossing (these paths can have tangencies). In a similar way, we define the sets $nw(k)$ for any k: they are the sets of all configurations of d directed non-crossing paths, going from north-west to south-east. The lth path goes from $DV_{k-1,l}$ to $DV_{k,l}$.

Now in order to prove Theorem 1, we start from the following observation, illustrated in Fig. 4: in $\mathscr{T}_{x,y}$ the distinguished vertices $DV_{k,l}$ are held fixed and one can consider *independent* patches of the families SW or NW, as follows. Without loss of generality, we focus on SW. We cut each path SW_k into $d+1$ sections, denoted by $SW_k(l)$, where $l=1,\ldots,d+1$. The section $SW_k(l)$ goes from $DV_{k,l-1}$ to $DV_{k,l}$. Then all the b sections $SW_k(l)$, $k=1,\ldots,b$ form a local path configuration denoted by $P_{SW}(l)$. It belongs to $sw(l)$. In a similar way, the corresponding grid patches defined with respect to the family NW are denoted by $P_{NW}(k)$ and belong to $nw(k)$. Therefore, when x and y are fixed, we have the natural inclusion

$$\mathscr{T}_{x,y}\subset\prod_{u=1}^{d+1}sw(u)\prod_{v=1}^{b+1}nw(v), \tag{14}$$

where the products are direct. We prove below that

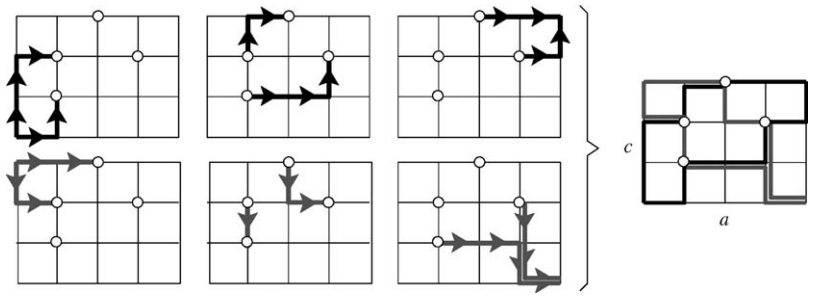

Fig. 5. Example of path concatenation involved in the proof of Lemma 1. The first line displays configurations from the sets $sw(u)$ (black paths). The second line from the sets $nw(v)$ (gray paths). Altogether, the superposition of the six patches forms a square grid representation. Black paths and gray paths can cross only at the distinguished vertices (white circles).

Lemma 1. *The previous inclusion is an equality*:

$$\mathscr{T}_{x,y} = \prod_{u=1}^{d+1} sw(u) \prod_{v=1}^{b+1} nw(v). \tag{15}$$

It follows from Eq. (15) that

$$\mathscr{T}_{a,c,b,d} = \bigcup_{(x,y)\in X\times Y}^{\text{disjoint}} \prod_{u=1}^{d+1} sw(u) \prod_{v=1}^{b+1} nw(v) \tag{16}$$

and that

$$T_{a,c,b,d} = \sum_{(x,y)\in X\times Y} \prod_{u=1}^{d+1} |sw(u)| \prod_{v=1}^{b+1} |nw(v)|. \tag{17}$$

The remainder of the proof consists in calculating the cardinalities $|sw(u)|$ and $|nw(v)|$ by the Gessel–Viennot method. Indeed, it is also demonstrated below that

Lemma 2. *When x and y are fixed*,

$$|sw(u)| = \det M^{(u)}(x,y); \qquad |nw(v)| = \det P^{(v)}(x,y). \tag{18}$$

Proof of Lemma 1. We need to prove the reverse inclusion

$$\mathscr{T}_{x,y} \supset \prod_{u=1}^{d+1} sw(u) \prod_{v=1}^{b+1} nw(v). \tag{19}$$

Configurations from the sets $sw(u)$ provide sections of paths from $DV_{k,l-1}$ to $DV_{k,l}$. When concatenated, these sections provide complete directed non-crossing paths from $(0,0)$ to (a,c), which form a family SW. In a similar way, sections from the $nw(v)$ provide directed non-crossing paths from $(0,c)$ to $(a,0)$, forming a family NW. We only need to check that any two paths from SW and NW only cross at the distinguished

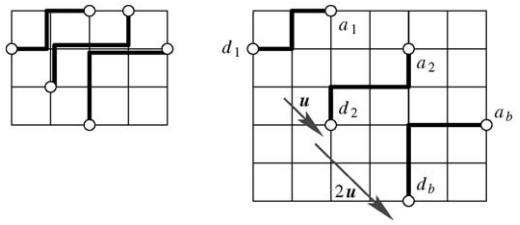

Fig. 6. Left: a configuration of non-*crossing* paths; Right: a configuration of non-*intersecting* paths. The second configuration is obtained from the first one via the shifts defined in the text. This correspondence is one-to-one.

vertices $DV_{k,l}$. This point is ensured by the directed character of path sections (see Fig. 5). This last observation is crucial and all the demonstration relies on it: it ensures the reverse inclusion and therefore the direct character of product (15), from which our enumerating formula ensues. □

Proof of Lemma 2. So far we have used the terminologies "non-*intersecting* paths" in Section 2 and "non-*crossing* paths" in Section 3. Now it is time to precise what aspects these two terms cover. We have seen that non-crossing paths can have tangencies, that is to say they can share vertices or edges of the grid, but they cannot step over one another. In particular, non-crossing paths of families SW (or NW) share their ends, but can be indexed from west to east without ambiguity.

On the contrary, non-intersecting paths cannot share any vertex or edge. Therefore, if we want to use the Gessel–Viennot method, we need to transform configurations of non-crossing paths on the square grid into configurations of non-intersecting paths. The trick consists in shifting non-crossing paths, as it is illustrated in Fig. 6. The trick is standard and was already used by Elnitsky [6] for example.

We use a unitary shift vector $\boldsymbol{u}=(1,-1)$ and we shift the kth path section $SW_k(l)$ by a vector $(k-1)\boldsymbol{u}$ (see the figure). The new paths still belong to the square grid. The kth new path section goes from the new vertex $DV'_{k,l-1}$ to the new vertex $DV'_{k,l}$, of coordinates

$$x'_{k,l}=x_{k,l}+(k-1) \quad \text{and} \quad y'_{k,l}=y_{k,l}-(k-1). \tag{20}$$

The so-obtained path configuration is non-intersecting by construction. This correspondence between configurations of non-crossing paths and configurations of non-intersecting paths is bijective.

Now we use the Gessel–Viennot technique by setting the departure vertices $d_i=DV'_{i,l-1}$ and the arrival ones $a_j=DV'_{j,l}$. The number of directed paths on the square grid going from a vertex $D=(x_D,y_D)$ to a vertex $A=(x_A,y_A)$ is simply given by the binomial coefficient

$$\lambda=\binom{x_A-x_D+y_A-y_D}{x_A-x_D}. \tag{21}$$

Then one computes the coefficients λ_{ij} involved in the Gessel–Viennot method: $\lambda_{ij} = m_{ij}$. Thus one obtains the matrices $M^{(u)}(x, y)$, the determinants of which count the elements of $sw(u)$. In the same way, to count the elements of the sets $nw(v)$, one must shift the sections of paths NW_l by $(l-1)\boldsymbol{v}$ where $\boldsymbol{v} = (1, 1)$. One gets the matrices $P^{(v)}(x, y)$ and takes their determinant, which completes the proof of Lemma 2. □

4. Conclusion

We have demonstrated how Elnitsky's technique can be generalized to octagons of any size, leading to an explicit enumerative formula (Theorem 1).

We also notice that conditions (5) and (6) (resp. (7) and (8)) that define the set X (resp. Y) are identical to the conditions defining plane partitions of height a (resp. c) on a $b \times d$ grid [10]. This point is remarkable because such plane partitions are known to be equivalent to rhombus tilings filling a centro-symmetric *hexagon* of sides lengths b, d and c (resp. b, d and a) [7]. We have derived a partial combinatorial interpretation of our formula (12) in terms of these tilings of hexagons. It is related to a natural decomposition of the configuration sets of tilings of octagons, as described in Ref. [4]. But it goes beyond the scope of the present paper and will be described elsewhere [5].

If $T^{\mathrm{hex}}_{a,b,c}$ denotes the number of tilings of the centro-symmetric hexagon of sides a, b and c, the previous remark leads to the lower bound

$$T_{a,b,c,d} \geqslant T^{\mathrm{hex}}_{b,d,c}\ T^{\mathrm{hex}}_{b,d,a}, \tag{22}$$

the number of terms the formula. By construction, the sets $nw(k)$ and $sw(l)$ are not empty and all terms are positive. In statistical physics and more specifically in quasicrystal science, people are interested in thermodynamic quantities such as the configurational entropy (per tile): $S = \ln(T_{a,b,c,d})/N_{\mathrm{T}}$ where N_{T} is the number of tiles. With our polygonal boundary conditions, this quantity has a finite limit when N_{T} goes to infinity provided the relative ratios of the side lengths also have a finite limit [3,4,7,11]. In the so-called "diagonal" case where all side lengths are equal, taking into account the number of tiles, the previous relation becomes $S \geqslant S^{\mathrm{hex}} = (\frac{3}{2})\ln 3 - 2\ln 2 \simeq 0.262$ [7]. The actual value of S is numerically known to be close to 0.36 [4]. The previous lower bound is manifestly loose and its improvement requires a better knowledge of the asymptotic behavior of the determinants in (12) at the large size limit.

But the main advantage of our formula precisely lies on the fact that the previous bound is weak: the formula realizes an exponential reduction of the number of terms as compared to a crude enumeration of tilings. Indeed, as it was just discussed in the previous paragraph, the number of terms grows exponentially like $\exp(0.26N_{\mathrm{T}})$ whereas the number of tilings grows like $\exp(0.36N_{\mathrm{T}})$. Even if in practice we cannot compute numerically the number of tilings of octagons bigger than in Table 1, the progress is already significant. Moreover, there exists some hope to simplify our formula, at least partially, as in Eq. (3).

In addition, the formula brings a new insight into the structure of tiling sets: it emphasizes a natural decomposition of the sets into smaller disjoint subsets, the cardinality of which is simply given by evaluation of determinants.

Acknowledgements

We are indebted to one of the referees for a careful reading of our manuscript and sound suggestions of improvements.

References

[1] N.G. de Bruijn, Algebraic theory of Penrose's non-periodic tilings of the plane, Kon. Nederl. Akad. Wetensch. Proc. Ser. A 84 (1981) 1–38.
[2] N.G. de Bruijn, Dualization of multigrids, J. Phys. France 47 (1986) C3–9.
[3] N. Destainville, Entropy and boundary conditions in random rhombus tilings, J. Phys. A 31 (1998) 6123–6139.
[4] N. Destainville, R. Mosseri, F. Bailly, Fixed-boundary octagonal random tilings: a combinatorial approach, J. Statist. Phys. 102 (2001) 147–190.
[5] N. Destainville, R. Mosseri, F. Bailly, in preparation.
[6] S. Elnitsky, Rhombic tilings of polygons and classes of reduced words in Coxeter groups, J. Combin. Theory A 77 (1997) 193–221.
[7] V. Elser, Solution of the dimer problem on a hexagonal lattice with boundary, J. Phys. A 17 (1984) 1509–1514.
[8] F. Gähler, J. Rhyner, Equivalence of the generalized grid and projection methods for the construction of quasiperiodic tilings, J. Phys. A 19 (1986) 267–278.
[9] I. Gessel, G. Viennot, Binomial determinants, paths and hook length formulae, Adv. Math. 58 (1985) 300–321.
[10] P.A. Mac Mahon, Combinatory Analysis, Cambridge University Press, Cambridge, 1916.
[11] R. Mosseri, F. Bailly, Configurational entropy in octagonal tiling models, Internat. J. Modern Phys. B 7 (6 & 7) (1993) 1427–1436.
[12] J.E.S. Socolar, P.J. Steinhardt, D. Levine, Quasicrystals with arbitrary orientational symmetry, Phys. Rev. B 32 (1985) 5547–5550.
[13] J.M. Stembridge, Non-intersecting paths, pfaffians, and plane partitions, Adv. Math. 83 (1990) 96–131.